Effects of Reactive Reinforced Interface on the Morphology and Tensile Properties of Amorphous Polyamide–SAN Blends

KILWON CHO,[1] KYUNG HOON SEO,[2] TAE OAN AHN[2]

[1] Department of Chemical Engineering and Polymer Research Institute, Center for Advanced Functional Polymers, Pohang University of Science and Technology, Pohang 790-784, Korea

[2] Department of Chemical Technology, Seoul National University, Seoul 151-742, Korea

ABSTRACT: The effects of reactive reinforced interface on the morphology and tensile properties of amorphous polyamide (a-PA) and styrene-acrylonitrile (SAN) copolymer blend have been investigated using styrene maleic anhydride (SMA) copolymer as a reactive compatibilizer. The anhydride groups of SMA copolymer can react with the amine groups of polyamide and form *in situ* graft copolymers at the a-PA–SAN interfaces during the blend preparation. The interfacial adhesion strength of the reactive reinforced interface was evaluated quantitatively using an asymmetric double cantilever beam fracture test as a function of SMA copolymer content using a model adhesive joint. The interfacial adhesion strength was found to increase with the content of SMA copolymer and then level off. The morphological observations of a-PA–SAN (80/20 w/w) blends showed that the finer dispersion of the SAN domains with rather narrow distribution was obtained by the addition of SMA copolymer into the blends. The trend of morphology change was not in accord with that of the interfacial adhesion strength with respect to the content of SMA copolymer. However, the results of tensile properties showed very similar behavior to the case of the interfacial adhesion strength with respect to SMA content; that is, there was an optimum level of the reactive compatibilizer beyond which the interfacial adhesion strength and tensile strength did not change significantly. These results clearly reveal that tensile properties of polymer blend are highly dependent on the interfacial adhesion strength. Furthermore, it is suggested that the asymmetric double cantilever beam fracture test using a model interface is a useful method to quantify the adhesion strength between the phases in real polymer blends. © 1998 John Wiley & Sons, Inc. J Appl Polym Sci 68: 1925–1933, 1998

Key words: reactive compatibilization; interfacial adhesion; tensile properties; polyamide; SAN copolymer

INTRODUCTION

Blending of different polymers is an effective way to develop advanced materials combining the useful properties of each polymer. However, most polymer blends are immiscible because of little mixing entropy available between polymers. This incompatibility often results in polymer blends having poor mechanical properties as compared with relevant polymers.

Much attention has been paid to the use of reactive compatibilizer to improve the mechanical properties and control the morphologies of immiscible polymer blends. The reactive compatibilizer has specific functional groups and it can generate

in situ formation of block or graft copolymers at the interface during the blend preparation through the reaction of functional groups incorporated onto the blend components.[1,2] The *in situ* formed copolymers at the interface provide a fine morphology and increase the interfacial adhesion strength between the phases. The reactive compatibilization method has been proved to be effective for controlling the morphology and improving the mechanical properties in a variety of blend systems.[3–6] However, the researches on the detailed understanding of the enhancement of interfacial properties resulting from the reactive compatibilization are limited.[7–11]

Recently, several studies[12–18] have been reported on the evaluation of reinforcement of polymer interfaces with a reactive compatibilizer using an asymmetric double cantilever beam (ADCB) fracture test by isolating the interface in a model adhesive joint. This method has been proven to be effective to evaluate the effect of reactive compatibilization quantitatively on the interfacial adhesion between immiscible polymers. Although the effects of reactive compatibilizer on the interfacial adhesion and mechanical properties have been studied by many researchers, the trial to correlate the interfacial adhesion strength with other properties, such as morphology and mechanical properties, is few.[18,19]

In this study, amorphous polyamide (a-PA) and styrene-acrylonitrile (SAN) copolymer were melt-blended using styrene-maleic anhydride (SMA) copolymer as a reactive compatibilizer in order to investigate the effects of interfacial adhesion on the morphology and tensile properties. The SMA copolymer is miscible with SAN copolymer,[20,21] and the a-PA–SAN interface would be reinforced by the *in situ* copolymer formation through the reaction between the terminal amine group of polyamide and the anhydride group of SMA copolymer. The content of SMA copolymer was varied in order to examine the effects of functional group concentration on the interfacial adhesion, morphology, and tensile properties of reactive blends. The enhancement of the interfacial adhesion strength was determined as a function of SMA copolymer content using the asymmetric double cantilever beam fracture test. Then, the interfacial adhesion strength was related to the tensile properties of the blends.

EXPERIMENTAL

Materials

The a-PA used in this study was CX-3000 obtained from the Unitika Company (Japan). The
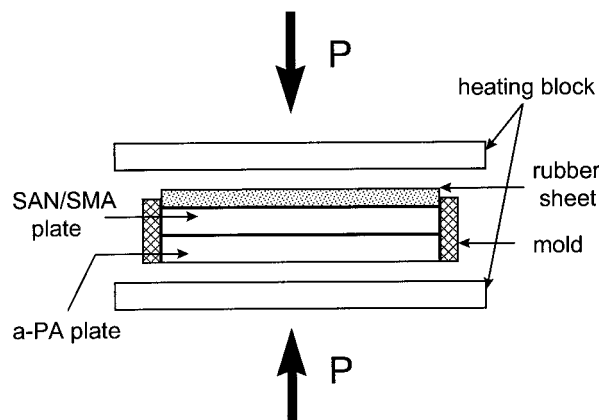

Figure 1 Technique used to bond the plates.

SAN containing 24 wt % acrylonitrile was a commercial molding grade, obtained from Cheil Industry (Korea), and has a weight-average molecular weight of 155,000 g/mol ($\bar{M}_w/\bar{M}_n = 2.16$). The SMA, used as a reactive compatibilizer in this study, was supplied by the DSM company and has a weight-average molecular weight of 110,000 g/mol. The SMA has 28 wt % maleic anhydride content and is reported to be miscible with SAN containing 24 wt % acrylonitrile.[20,21]

Melt Blending

The polymers used in this study were dried under vacuum at 80°C for 24 h before melt blending. Amorphous polyamide—SAN–SMA blends were prepared in two steps. First, SAN–SMA blends with different composition were made by melt mixing in an internal mixer (Brabender Plasticorder) at speed of 50 rev min^{-1}. The mixer temperature was set at 200°C. The prepared SAN–SMA blends were subsequently melt blended with a-PA in an internal mixer under the same condition. The final a-PA—(SAN–SMA) blend ratio was 80/20 w/w.

Interfacial Adhesion Strength Measurement

SAN–SMA blend and a-PA were compression-molded into plates of 2 mm thickness using a hot press. The molding temperature was 200°C. To obtain smooth glossy molding surface, a polished Ferrotype plate was used as a molding plate. The molded plates were stored in vacuum oven to prevent any possible contamination. Then the two molded plates were joined in a hot press at 180°C for 1 h (Fig. 1). Light pressure was exerted on the plates to promote good contact between the
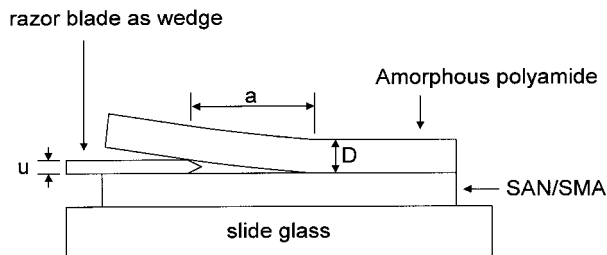
Figure 2 Schematic diagram for the asymmetric double cantilever beam fracture test specimen.

two surfaces. The joined specimens were allowed to cool slowly in the mold and then cut into strips of 5 mm in width using a diamond saw.

The adhesive joint specimens were fractured at room temperature to measure the critical strain energy release rate G_C, using an asymmetric double cantilever beam (ADCB) fracture test, which drives the crack along the interface. The SAN–SMA blend plate, which has lower yield stress, was adhered to a glass slide, then the crack was propagated by inserting a razor blade into the interface. The crack induced by a razor blade was allowed to propagate slowly for 24 h before measurement. The crack length was measured using a travelling microscope. The schematic diagram of the ADCB fracture test is shown in Figure 2. The interfacial fracture toughness G_C was calculated by the following equation[22]:

$$G_C = 3ED^3u^2\{8a^4(1 + 0.64D/a)^4\}^{-1}$$

where E is the modulus, D is the thickness of specimen, u is the thickness of razor blade, and a is the crack length propagated.

To study the failure mode and the locus of failure, the fracture surfaces were examined using a scanning electron microscope (Jeol JSM-840A). In all experiments, matching sides of the fractured specimens were examined.

Morphology and Tensile Properties

Morphology of the melt blend was examined with a scanning electron microscope. The specimen was frozen in liquid nitrogen and immediately fractured. The dog bone shaped tensile test specimens of 0.65 mm in thickness were prepared by compression molding at 200°C, subsequently quenched to room temperature with water circulation in a hot press. Tensile strength and strain were measured according to ASTM D 1708 using an universal testing machine (Instron Model 4206) at a crosshead speed of 5 mm/min at room temperature. At least 8 specimens of each sample were used, and the average values of tensile strength at break and ultimate elongation were obtained. The tensile fractured specimens were cut parallel to the direction of tension by the razor blade to observe the morphological change of dispersed phase in tensile test. The cut surface of the tensile tested specimen was examined with a scanning electron microscope.

RESULTS AND DISCUSSION

Interfacial Adhesion

In this study, SMA copolymer containing 28 wt % maleic anhydride was chosen as a reactive compatibilizer in a-PA–SAN system because the SMA copolymer is miscible with the SAN copolymer containing 24 wt % acrylonitrile used in this study.[20,21] The amine end group of a-PA reacts with the anhydride group of SMA copolymer and forms an imide bond at the a-PA–SAN interface. This imide bond will bridge the two phases and improve the interfacial adhesion strength. The content of SMA copolymer in SAN–SMA blends was varied to change the interfacial adhesion strength by controlling the number of interlinking chains across the interface. The schematic diagram of *in situ* copolymer formation at the interface is shown in Figure 3.
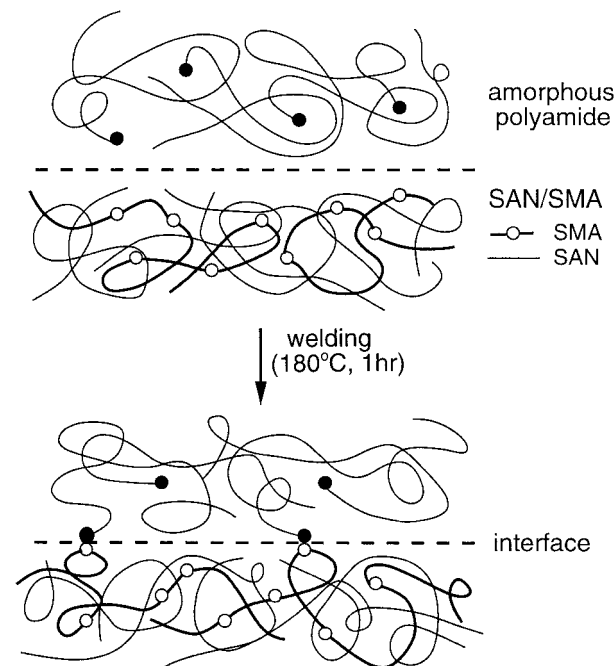

Figure 3 Schematic diagram of *in situ* copolymer formation at a-PA—(SAN–SMA) interface: (●) amine group of a-PA; (○) anhydride group of SMA.
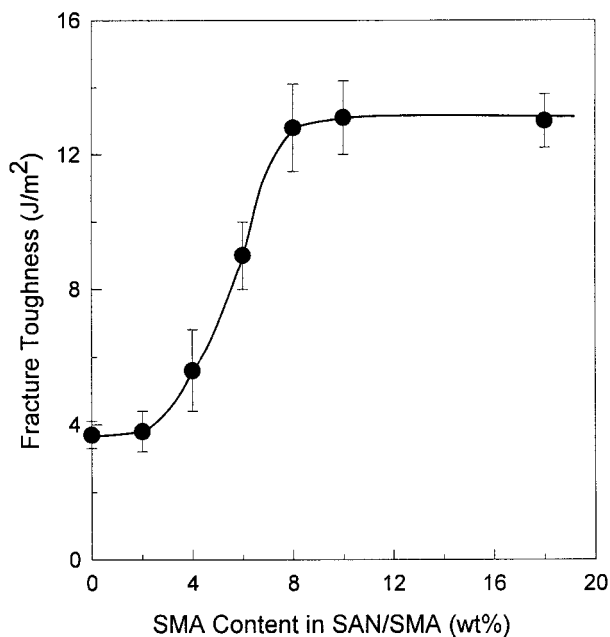
Figure 4 Interfacial fracture toughness G_C as a function of SMA content in SAN–SMA.

Results of fracture toughnesses of a-PA–SAN interface as a function of the content of SMA copolymer in SAN–SMA blend are presented in Figure 4. The interfacial fracture toughness of a-PA–SAN adhesive joint without any SMA copolymer was about 3.7 J/m^2. This value is quite low, which implies that there is little chain entanglement between a-PA and SAN copolymer because the system is not thermodynamically miscible. The fracture toughness was found to increase with the amount of SMA copolymer and then level off at 8 wt % SMA copolymer content in SAN–SMA blend. The saturated value of interfacial fracture toughness was around 13 J/m^2. The experimental results of increasing fracture toughness with increasing amount of SMA copolymer is well in accord with other reported results.[12-16] This result is consistent with the concept that the interfacial fracture toughness is highly dependent on the number of interlinking chains crossing a given interface, a concept that has been well established in a model study using a diblock copolymer as a compatibilizer.[23-25]

Since the higher concentration of the anhydride group in SAN–SMA blend has more probability of forming chemical bonds with the terminal amine group of a-PA, one would expect that the higher content of SMA copolymer produces the more interlinking chains at the interface. This means that the interfacial fracture toughness would increase with increasing number of interlinking chains. However, above 8 wt % of SMA copolymer in SAN–SMA blend further increase of SMA copolymer content could not increase the number of interlinking chains formed at the interface any more. This is due to the limited availability of the terminal amine groups of a-PA, although there was an overabundance of anhydride group. Therefore, the number of interlinking chains per unit area of interface became saturated around 8 wt % of SMA content, which resulted in saturation of interfacial adhesion strength.

Yukioka and Inoue[9] measured the interfacial thickness between amorphous polyamide and the blend of SAN and SMA using ellipsometric analysis. Here, the acrylonitrile content of SAN was 25 wt % and the maleic anhydride contents of SMA was 23 wt %. Their system is very similar to ours, and the results can be referred to this system. According to their results, with increasing SMA content, the interfacial thickness increased, attained a maximum, and then decreased. The maximum thickness of 50 nm was attained when the SMA content was slightly less than 10 wt %. As the interfacial thickness increased, the number of interlinking molecules increased. Therefore, the maximum number of interlinking molecules was attained around 10 wt % of SMA content from their results. This saturation SMA content is well consistent with our results of interfacial fracture toughness. So it is supposed that the saturation interfacial thickness of our system is about 50 nm.

It is worth noting that the effect of migration of small chains of SMA copolymer to the interface on the interfacial properties, such as interfacial adhesion strength. The SMA copolymer has a broad molecular weight distribution. Thus, small molecular chains tend to migrate to the interface and react with the terminal amine groups of a-PA. Thermodynamically, the migration of small molecules to the interface is favored in polydisperse systems. For example, Broseta et al.[26] reported that in polydisperse systems, small chains accumulate slightly at the interface and slightly lower the interfacial tension. However, the accumulation of small chains at the interface was found to be very slight. Furthermore, the equilibration time of the polymer melt needed for the surface segregation of small molecules in polydisperse systems depends on the temperature, and generally the time is tens of hours because of high viscosity, that is, the lower mobility of the polymer melt. In our a-PA–(SAN–SMA) system, although the migration of small chains of SMA copolymer to the interface is favored thermodynamically, the migration is restricted by the low mobility of poly-

mer melt due to the relatively low welding temperature. Moreover, the *in situ* formed copolymers at the interface hinder the migration of the smallest SMA chains to the interface. Therefore, it is supposed that the role of the smallest SMA chains at the interface to influence the interfacial properties is minor.

It is also noteworthy that the interfacial fracture toughness of a-PA–SAN adhesive joint was relatively low, that is, a few J/m^2. Even the saturated value of adhesion strength was only about 13 J/m^2. This value is quite low as compared with the fracture energy of the relevant homopolymer, that is, more than few hundreds J/m^2. This low value is associated with the low-energy losses during the deformation at the crack tip.[27,28] At the saturation point, the amount of interlinking bond across the a-PA–SAN interface is large. However, the breaking strength of interlinking bonds across the interface is lower than the yield stress of a-PA (105 MPa) or SAN copolymer (68 MPa); that is, the strength of interlinking molecules is not strong enough to induce the plastic deformation of the adherand, such as a-PA or SAN copolymer, which results in the low-energy losses during the crack propagation. Therefore, the interfacial fracture toughness of the reactive reinforced a-PA–SAN adhesive joint is relatively low, even at the saturation point.

To ascertain the failure mode, the fracture surfaces after interfacial adhesion strength measurement were examined by a scanning electron microscope. Even at the saturation point, any plastic deformation was not observed in both a-PA and SAN–SMA fracture surfaces, as expected. Therefore, the microscopic observation supports the result of low interfacial adhesion strength at the saturation point.

Morphology Studies

The effects of the reactive compatibilizer, that is, the SMA copolymer, on the morphology of the a-PA–SAN blend are shown in Figure 5. For a-PA–SAN (80/20) blends, spherical particles of SAN copolymer domains were dispersed in a-PA continuous phase. Figure 5 shows the average domain size of a-PA—(SAN–SMA) blend as a function of the content of SMA copolymer in SAN–SMA. The error bar at each point is the standard deviation of the measured domain size. When the SMA copolymer was not present in the blend, the average size of the dispersed domain was about 1.8 μm and the distribution of domain size was broad. However, when the SMA copolymer was
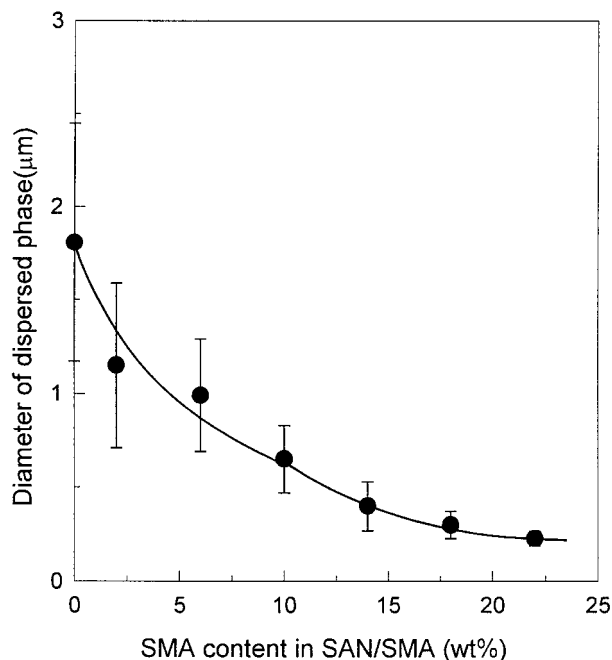

Figure 5 Diameter of the dispersed phase in a-PA—(SAN–SMA) 80/20 blends as a function of SMA content in SAN–SMA.

added into the a-PA–SAN blend, the domain size significantly decreased to the order of 0.2 μm. Moreover, the distribution of domain size became narrower with the increasing SMA copolymer content in SAN–SMA blend. It can be explained by two reasons. One is the reduced interfacial tension due to the presence of *in situ* formed graft copolymers at the interfaces because the size of dispersed phase is proportional to the interfacial tension.[29] Many researchers[7,8] have reported that the reduction of interfacial tension by reactive blending is similar to the case of block copolymer addition to immiscible polymer blends.

However, the decreasing breadth of the domain size distribution with increasing SMA copolymer content cannot be explained by the reduction of interfacial tension alone. Although the average domain size of uncompatibilized system was large, very small domains also appeared. The small domain size cannot be explained in principle by the interfacial tension. It means that the phase coalescence is also an important factor in determining the final blend morphology in the melt blending, as already reported by many researchers.[30–32] In the case of uncompatibilized system, a very small domain may result from the breakup process in the high shear regions, while increased coalescence due to more interaction of domains will result in very large size domains.[33]

However, in the case of reactive compatibilized system, that is, the blends with SMA copolymer in this study, the coalescence is prevented in the blending because the *in situ* formed graft copolymers at the interface may form an interphase, which must be overcome for coalescence to occur.[33] As a result, with increasing SMA copolymer content in SAN–SMA blends, the breadth of domain size distribution became narrower due to the suppression of phase coalescence between the small domains, as shown in Figure 5.

In the case of interfacial fracture toughness, the value was saturated above 8 wt % SMA copolymer content in SAN–SMA blend. However, the domain size continuously decreased with increasing SMA copolymer content up to 20 wt % in SAN–SMA blend. This result is not in accord with the result of interfacial adhesion strength with respect to the content of SMA copolymer. The different behavior is due to the different experimental conditions. In the experiment for interfacial fracture toughness measurement, the significant mixing of a-PA and SAN copolymer molecules did not occur at the interface; that is, the reaction between anhydride and amine groups took place at the interface without severe mixing of relevant polymer molecules. However, in the case of melt blending by an internal mixer, significant mixing of the two polymer molecules took place, and the possibility of forming copolymers was higher than that of the case without mixing because the complex rheological forces broke large dispersed phase into the small one and thus made large interfacial area contacting the two phases. Therefore, in the melt blending the reaction between reactive groups can proceed further if there exists anhydride functional groups. Thus, the domain size continuously decreased with increasing SMA copolymer content even above 8 wt % SMA copolymer content in SAN–SMA.

Although the extent of reaction in the case of melt blending was higher as compared with the interfacial adhesion experiments due to larger overall interfacial area, the number of interlinking chains per unit area of interface was, however, expected to be similar in each case because the interfacial fracture toughness did not increase further once the value reached the saturated value. It was supported by the tensile properties of blends, described in the later section.

As the number of interlinking chains per unit area of interface was saturated above 8 wt % of SMA copolymer in SAN–SMA, the interfacial tension would not decrease further. Therefore, the decrease of the domain size after the saturation point cannot be explained by the reduction of interfacial tension alone. It indicates that the suppression of phase coalescence due to the formed copolymer at the interface significantly affects the size of dispersed phase. As a result, the morphology variation with content of reactive compatibilizer seems to show different behavior from that of interfacial adhesion strength.

Tensile Properties

The results of the tensile tests for the blends of a-PA—(SAN–SMA) 80/20 w/w are presented in Figure 6 as a function of the content of SMA copolymer in SAN–SMA. The tensile strength and elongation at break increased as increasing amount of SMA copolymer in SAN–SMA and then leveled off around 10 wt % SMA copolymer content. This behavior is very similar to the results of interfacial fracture toughness. It is reported that the tensile properties of polymer blends are very sensitive to the state of the interface,[34,35] that is, interfacial adhesion, because the tensile strength is governed by the flaw in the specimen.[36] The poor interface behaves as a flaw, and the failure initiates at the interface, which results in low tensile strength. The enhancement of interfacial fracture toughness with increasing content of SMA copolymer, as already shown in Figure 4, contributed to the improvement of tensile properties.

In general, the mechanical properties of polymer blends are also highly dependent on the morphology as well as the interfacial adhesion. However, in the case of multiphase polymer alloys, the ultimate mechanical responses, such as tensile strength and elongation at break, are more affected by the internal flaw, which is closely related to the interfacial adhesion, although some other properties, such as impact strength, are much affected by morphology. Therefore, considering that the effect of morphology on the tensile properties is not significant in the case of weak interfacial adhesion, the comparison between the interfacial adhesion and the tensile properties can be made. This also indicates that the interfacial adhesion strength quantified by the ADCB fracture test using a model interface reflects considerably well the real interfacial adhesion between the continuous phase and the dispersed phase in a real blend system.

To ascertain the correlation between the tensile properties and the interfacial fracture toughness, the morphological changes of the dispersed phase after tensile test were examined with a scanning
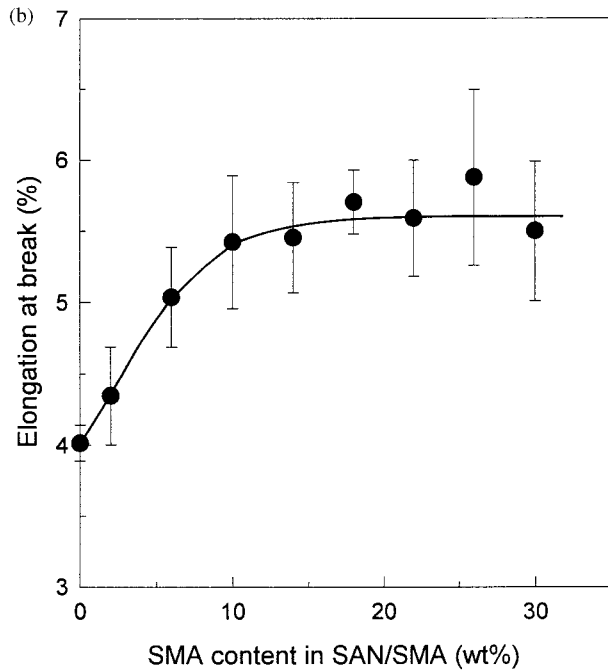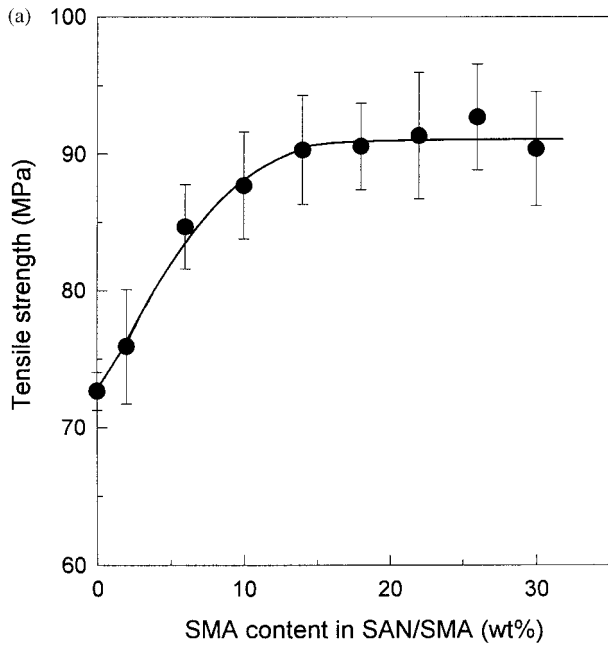
(a)

(a)

(b)

(b)

Figure 6 (a) Tensile strength and (b) elongation at break of a-PA—(SAN–SMA) 80/20 blends as a function of SMA content in SAN–SMA.
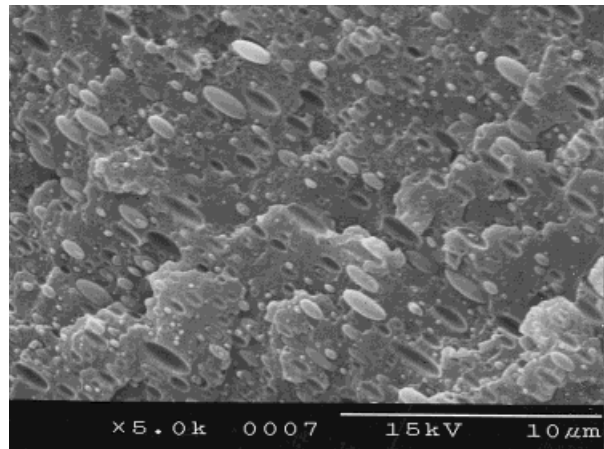
electron microscope. The micrographs are shown in Figure 7 for various SMA copolymer contents (0, 6, and 10 wt %) in SAN–SMA blend. It is noted that a-PA and SAN copolymer show ductile behavior. As can be seen in Figure 7(a), when SMA copolymer was absent, large cavities were clearly observed at the a-PA–SAN interface; that is, the interfacial failure occurred because the in-
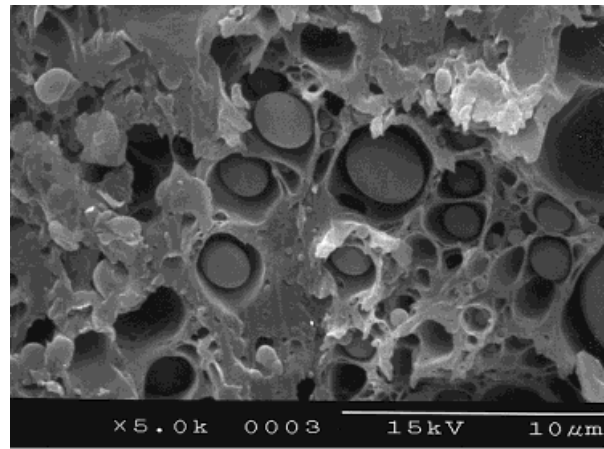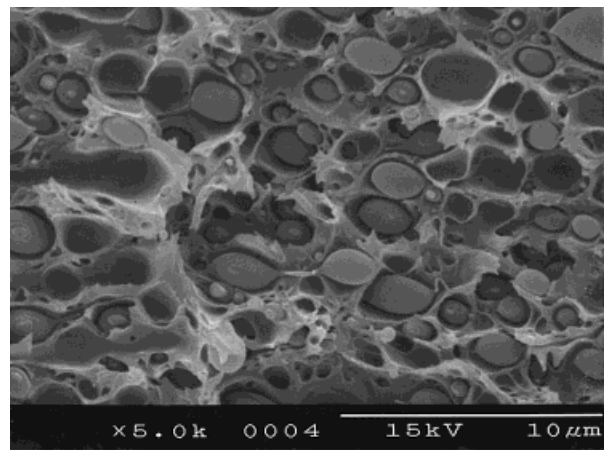
(c)

Figure 7 Scanning electron micrographs showing deformation of the dispersed phase after tensile test: (a) 100/0; (b) 94/6; and (c) 90/10 w/w SAN–SMA for a-PA—(SAN–SMA) 80/20 blends.

terfacial adhesion strength was very weak, as shown in Figure 4. By the tensile elongation, the ductile a-PA matrix was deformed severely, while the SAN–SMA domains were hardly deformed because of no stress transfer between the two phases due to the weak interfacial adhesion. In this case, the poor interface behaved as a flaw, and the failure initiated at the interface, which resulted in the poor tensile strength and the low elongation at break. When the SMA content was 6 wt %, the interface between the two phases also failed. However, the dispersed domains were deformed slightly, as shown in Figure 7(b). This was caused by the stress transfer between the two phases, and this result indicated that the interfacial adhesion strength was improved when SMA was present. However, the interfacial adhesion strength was not strong enough to prevent the crack initiation at the a-PA—(SAN–SMA) interface.

The morphological changes of the dispersed phases after the tensile test for the blend containing 10 wt % of SMA copolymer are shown in Figure 7(c). In contrast to the other micrographs [Fig. 7(a) and 7(b)], the interface did not fail during the tensile test. Also, the dispersed domains were deformed severely due to the stress transfer between the two phases. This result indicated that the interfacial adhesion strength was improved to the degree at which it prevents the crack initiation at the a-PA—(SAN–SMA) interface. Therefore, the tensile strength and the elongation at break were saturated when the SMA copolymer content in SAN–SMA blend reached 10 wt %. Further increase of SMA copolymer content in SAN–SMA blend did not improve the interfacial adhesion strength and so the tensile properties were leveled off, although the sizes of dispersed domains decreased continuously.

CONCLUSIONS

The addition of SMA copolymer into a-PA–SAN system led to the enhancement of interfacial fracture toughness measured by the ADCB fracture test using a model interface. The interfacial fracture toughness increased as increasing SMA copolymer content and then saturated at 8 wt % SMA copolymer content in SAN–SMA blend. Further increase of SMA copolymer content in SAN–SMA blend could not improve the interfacial fracture toughness because there was an overabundance of the anhydride groups. However, the size of the dispersed phase in the melt blend continuously decreased after the saturation point. This result shows that the final morphology of reactive blend can be controlled not only by the reduction of interfacial tension but also by the suppression of phase coalescence, which is originated from the *in situ* formed copolymer at the interface. Therefore, the result of interfacial fracture toughness cannot be related directly to the morphology behavior of melt blend.

The tensile properties of a-PA—(SAN–SMA) 80/20 w/w melt blends were also improved by the addition of SMA copolymer. The tensile properties increased with the amount of SMA copolymer in SAN–SMA blend and then saturated around 10 wt % SMA copolymer content in SAN–SMA blend. This behavior is very similar to that of interfacial fracture toughness because the tensile properties of multicomponent polymer blends are highly dependent on the interfacial adhesion strength. From these results, it is concluded that the ADCB fracture test by isolating the interface in a model fracture geometry was found to be a useful method to characterize the interfacial adhesion strength between the continuous phase and the dispersed phases in real polymer blend.

REFERENCES

1. M. Xanthos and S. S. Dagli, *Polym. Eng. Sci.,* **31,** 929 (1991).
2. N. C. Liu and W. E. Baker, *Adv. Polym. Technol.,* **11,** 249 (1992).
3. J. C. Angola, Y. Fujita, T. Sakai, and T. Inoue, *J. Polym. Sci., Polym. Phys. Ed.,* **26,** 807 (1988).
4. C. Koning, A. Ikker, R. Borggreve, L. Leemans, and M. Moller, *Polymer,* **34,** 4410 (1993).
5. B. Majumdar, H. Keskkula, and D. R. Paul, *Polymer,* **35,** 3164 (1994).
6. J. W. Lee, Y. S. Seo, S. S. Hwang, K. U. Kim, and S. I. Hong, *Polymer (Korea),* **16,** 39 (1992).
7. K. Cho, H. K. Jeon, C. E. Park, J. Kim, and K. U. Kim, *Polymer,* **37,** 1117 (1996).
8. C. A. Fleischer, A. R. Marales, and J. T. Koberstein, *Macromolecules,* **27,** 379 (1994).
9. S. Yukioka and T. Inoue, *Polymer,* **35,** 1182 (1994).
10. C. Scott and C. Macosko, *J. Polym. Sci., Polym. Phys. Ed.,* **32,** 205 (1994).
11. W. E. Baker and N. C. Liu, *ACS Polym. Prepr.,* **34,** 787 (1993).
12. E. Boucher, J. P. Folkers, C. Creton, H. Hervet, and L. Leger, *Macromolecules,* **30,** 2102 (1997).
13. N. C. Beck Tan, D. G. Peiffer, and R. M. Briber, *Macromolecules,* **29,** 4969 (1996).
14. L. J. Norton, V. Smigolova, M. U. Pralle, A. Hu-

benko, K. H. Dai, E. J. Kramer, S. Hahn, C. Berglund, and B. DeKoven, *Macromolecules,* **28,** 1999 (1995).

15. K. Cho, K. H. Seo, T. O. Ahn, J. Kim, and K. U. Kim, *Polymer,* **38,** 4825 (1997).
16. E. Boucher, J. P. Folkers, H. Hervet, L. Leger, and C. Creton, *Macromolecules,* **29,** 774 (1996).
17. J.-E. Bidaux, G. D. Smith, N. Bernet, J.-A. E. Manson, and J. Hilborn, *Polymer,* **37,** 1129 (1996).
18. N. C. Beck Tan, S.-K. Tai, and R. M. Briber, *Polymer,* **37,** 3509 (1996).
19. M. Saleem and W. Baker, *J. Appl. Polym. Sci.,* **39,** 655 (1990).
20. Y. Aoki, *Macromolecules,* **21,** 1277 (1988).
21. J. Kressler, H. W. Kammer, G. Schmidt-Naake, and K. Herzog, *Polymer,* **29,** 686 (1988).
22. H. R. Brown, *J. Mater. Sci.,* **25,** 2791 (1990).
23. E. J. Kramer, L. J. Norton, C.-A. Dai, Y. Sha, and C.-Y. Hui, *Faraday Discuss,* **98,** 31 (1994).
24. C. Creton, E. J. Kramer, C.-Y. Hui, and H. R. Brown, *Macromolecules,* **25,** 3075 (1992).
25. K. Cho, T. O. Ahn, H. S. Ryu, and K. H. Seo, *Polymer,* **37,** 4849 (1996).
26. D. Broseta, G. H. Fredrickson, E. Helfand, and L. Leibler, *Macromolecules,* **23,** 132 (1990).
27. L. Mullins, *Trans. Inst. Rubb. Ind.,* **35,** 213 (1959).
28. K. A. Grosch, J. A. C. Harwood, and A. R. Payne, *Nature,* **212,** 497 (1966).
29. S. Wu, *Polym. Eng. Sci.,* **27,** 335 (1987).
30. G. I. Taylor, *Proc. R. Soc. London,* **A146,** 501 (1934).
31. B. D. Favis and J. M. Willis, *J. Polym. Sci., Polym. Phys. Ed.,* **28,** 2259 (1990).
32. F. M. Mirabella Jr., *J. Polym. Sci., Polym. Phys.,* **32,** 1205 (1994).
33. U. Sundararaj and C. W. Macosko, *Macromolecules,* **28,** 2647 (1995).
34. A. Legros, P. J. Carreau, B. D. Favis, and A. Michel, *Polymer,* **35,** 758 (1994).
35. A. J. Oshinski, H. Keskkula, and D. R. Paul, *Polymer,* **33,** 284 (1992).
36. E. H. Andrew, D. Barnard, M. Braden, and A. N. Gent, in *The Chemistry and Physics of Rubberlike Substances,* L. Bateman, Ed., Wiley, New York, 1963, Chap. 12.